Journal of Mathematical Chemistry 15 (1994) 157–181

The characterisation of coordination polyhedra by invariants

H. Terrones [1] and A.L. Mackay

Department of Crystallography, Birkbeck College, University of London, Malet Street, London WC1E 7HX, UK

Received 22 October 1992

We have extended the use of the invariants of spherical harmonics for the characterisation of the angular distribution of coordinating atoms about a central atom. These invariants are suitable indices for use in clustering algorithms for automatic crystal chemistry. Invariants for coordination polyhedra in intermetallic compounds and Ca–O silicates are considered. A study of invariants in coordination polyhedra distorted by the Jahn-Teller effect is presented. In addition, Invariants from small clusters and the cuboctahedron–icosahedron transition are analyzed.

1. Introduction

Steinhardt et al. [25] have developed a method of "shape spectroscopy" which can be applied in various ways for characterising bond orientational order in finite coordination polyhedra or extended arrays. Bunge [3] had earlier applied similar methods, much less lucidly, to metallic textures.

The method is based on the expression of the directional distribution, represented first as a distribution of density on the surface of a sphere, as spherical harmonics. These are calculated with respect to an arbitrary system of axes and then a series of invariants (invariant with respect to rotation of these arbitrary axes) can be further calculated. The invariants use the methodology developed for the addition of angular momenta in quantum mechanics [15]. A string of invariants of increasing order can be defined. Steinhardt et al. used the first two orders. We have examined also the next order. Sattinger used Lie algebra of infinitesimal generators of the rotation group for obtaining higher orders of invariants [22]. Times for computation rise rapidly with complexity.

The possibility of the construction of invariants arise from the rules for the com-

[1] Present address: Instituto de Física, UNAM, Apartado Postal 20-364, C.P. 01000 México, D.F., Mexico.

bination of zonal harmonics (with different axes) effectively by resolution of their components in a particular direction, summing over the tesseral harmonics.

The invariants of spherical harmonics can be seen to parallel the invariants of structure factors (with respect to crystallographic axes) developed by Karle [14] and Hauptmann [9] for solving crystal structures by direct methods. In the study of biomolecules by small-angle scattering this can have important application [28].

Invariants can be connected with the Landau theory of freezing for the energy of structures [13]. They are connected also with the choice of angles for the "double magic angle spinning" technique in NMR spectroscopy whereby spinning about two icosahedral axes has been shown to be superior to spinning about the two angles which represent the second and fourth zeros of the associated Legendre polynomial (54.7° *and* 30.6°) [31].

We have applied the invariants under rotation to characterise coordination polyhedra in intermetallic compounds in Ca–O silicates (O ions about the Ca). The behaviour of the invariants for coordination polyhedra distorted by the Jahn-Teller effect is also analyzed; here, we find that the most symmetric (most stable) structure is easy to identify. Steinhardt et al. [25] have calculated the invariants from some small clusters. In this paper we have extended the study to other clusters generated by the Monte Carlo method. We show that the quasicrystalline cluster proposed by Romeu [20] is highly icosahedral. Finally, we study how the invariants change during the cuboctahedron–icosahedron transformation.

In order to represent the results obtained by the invariants, a standard clustering program is used [24]. This program calculates generalized distances between all pairs of objects to be clustered and a tree diagram or dendrogram is then plotted to show similarities and differences. This method has been tried and found to be very satisfactory for showing differences in shape.

2. Spherical harmonics

The distribution of some variable over the surface of a sphere can be described by a series of orthogonal functions, calculated with respect to particular axes, usually the spherical coordinates (r, θ, ϕ), (with their origin at the centre of the sphere). The usual functions are the angular parts $Y_{lm}(\theta, \phi)$, called spherical harmonics [18]. Where $|m| \leqslant l$. The dependence of the variable on r will be ignored here for the moment since in our calculation of invariants just directions are considered. The spherical harmonics can be put as

$$Y_{lm}(\theta, \phi) = \sqrt{\frac{(2l+1)(l-m)!}{4\pi(l+m)!}} P_l^m(\cos\theta) e^{im\phi}, \tag{1}$$

where $P_l^m(\cos\theta)$ is the associated Legendre polynomial. We have used the program given by "Numerical Recipes" [19] for calculating the latter. When $m = 0$ the sphe-

rical harmonics divide a sphere into zones by sets of parallel circles; these harmonics are called zonal harmonics. If $m = l$ the sphere is divided into perpendicular sectors through the points $\theta = 0$ and $\theta = \pi$; these harmonics are called sectorial. When $0 < m < l$ the sphere is divided into two sets of circles which correspond to the zonal and sectorial harmonics; these are the tesseral harmonics. In order to show how the symmetry changes by choosing different spherical harmonics, we have calculated $\sum_m Y_{l,m}$ for different $l's$ (see fig. 1).

The coefficients of the various terms change as the axes are rotated, but it is possible to calculate quantities which are invariant with respect to this rotation and which thus can be used to characterise distributions which occur in different orientations. A series of invariants can be defined. We have used three which we have called, (after Steinhardt et al. [25]) Q, W and Z invariants.

3. Q invariants

Given a series of terms Y_{lm}, each the sum of the contributions of N atoms for a particular polyhedron, invariants can be calculated as follows [25]:

$$Q_{lm} = \frac{1}{N} \sum_{\text{bonds}} Y_{lm}\,, \tag{2}$$

$$Q_l = \left[\frac{4\pi}{2l+1} \sum_{m=-l}^{m=+l} |Q_{lm}|^2 \right]^{1/2} . \tag{3}$$

Thus, there is a Q invariant for each value of l.

Regarding the number of bonds, two different criteria are applied, one, for coordination polyhedra (CP) and the other, for clusters or small aggregates. In the case of CP we have an atom surrounded by its first neighbours which form a coordination shell, so the bonds used in eq. (3) are the lines joining the central atom with each first neighbour. In other words, the number of bonds is equal to the coordination number (number of first neighbours). Here, the bonds are directed from the central atom. On the other hand, for small clusters we will consider all the bonds in the cluster which have lengths less than or equal to a certain value, for example $1.2r_0$ where r_0 is the minimum distance between two atoms [8]. In the latter case, the bonds are undirected, so that the Q invariants for odd values of l change when the direction of the bond changes, but the even values remain the same since these are invariant under inversion.

4. W invariants

The expression for the W invariants is [25]

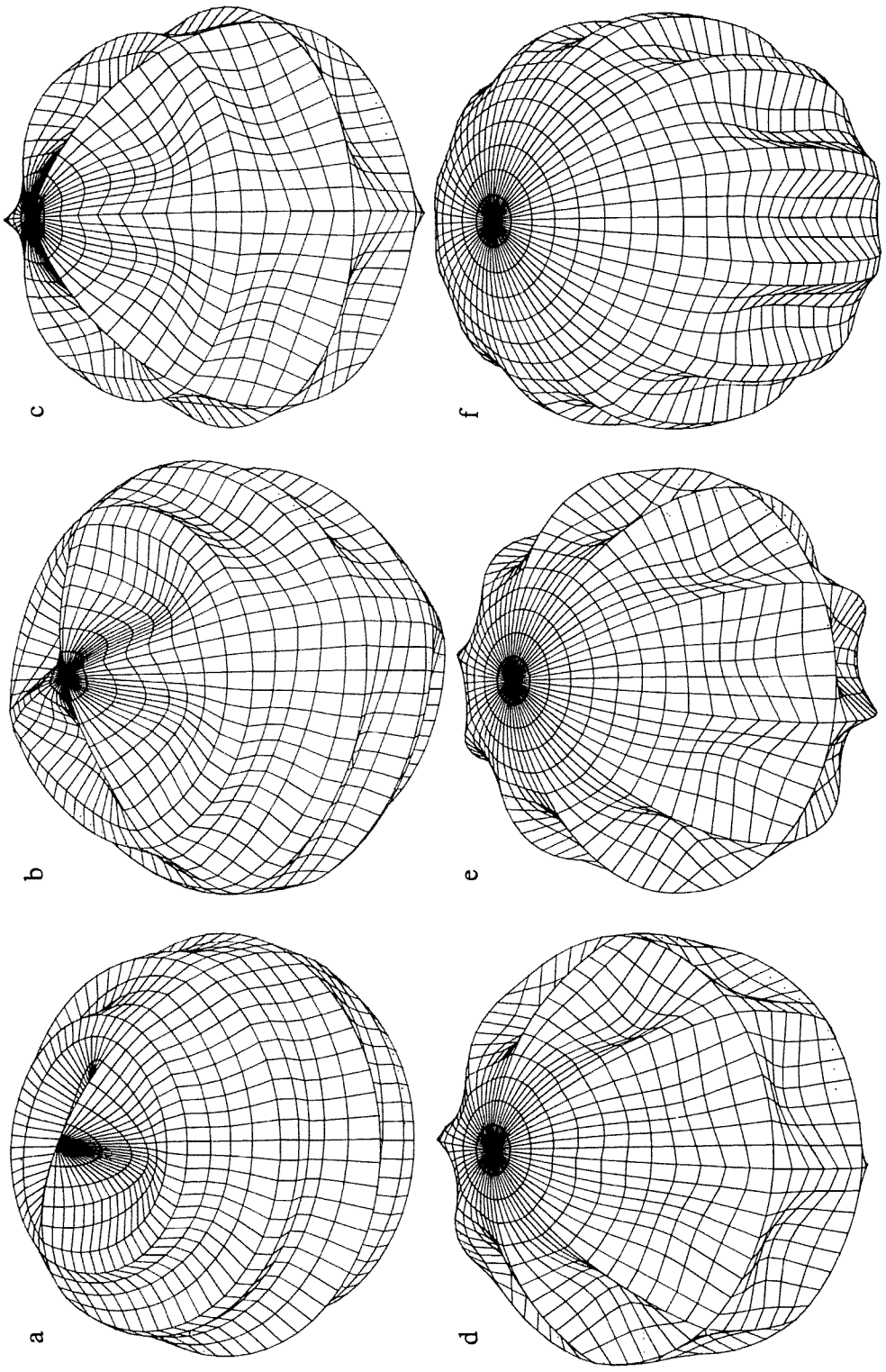

Fig. 1. Different spherical harmonics on the sphere showing different symmetries. (a) $|Y_{61} + Y_{6-1}|$. (b) $|Y_{62} + Y_{6-2}|$. (c) $|Y_{63} + Y_{6-3}|$. (d) $|Y_{64} + Y_{6-4}|$. (e) $|Y_{65} + Y_{6-5}|$. (f) $|Y_{66} + Y_{6-6}|$.

$$W_l = \frac{\sum_{\substack{m_1,m_2,m_3 \\ m_1+m_2+m_3=0}} \begin{pmatrix} l & l & l \\ m_1 & m_2 & m_3 \end{pmatrix} Q_{lm_1} Q_{lm_2} Q_{lm_3}}{\left[\sum_m |Q_{lm}|^2\right]^{3/2}}, \tag{4}$$

where the coefficients

$$\begin{pmatrix} l & l & l \\ m_1 & m_2 & m_3 \end{pmatrix} \tag{5}$$

are the 3-j Wigner symbols, used in quantum mechanics in the addition of angular momenta [15]. The explicit general form of this symbol can be written as

$$\begin{aligned} \begin{pmatrix} l_1 & l_2 & l_3 \\ m_1 & m_2 & m_3 \end{pmatrix} &= \left[\frac{(l_1+l_2-l_3)!(l_1-l_2+l_3)!(-l_1+l_2+l_3)!}{(l_1+l_2+l_3+1)!}\right]^{1/2} \\ &\times [(l_1+m_1)!(l_1-m_1)!(l_2+m_2)!(l_2-m_2)!(l_3+m_3)!(l_3-m_3)!]^{1/2} \\ &\times \sum_z (-1)^{z+l_1-l_2-m_3} / [z!(l_1+l_2-l_3-z)!(l_1-m_1-z)! \\ &\times (l_2+m_2-z)!(l_3-l_2+m_1+z)!(l_3-l_1-m_2+z)!] \end{aligned} \tag{6}$$

The summation is over all integers z but, since the factorial of a negative number is infinite the sum contains only a finite number of terms. We must recall that $0! = 1$. Talman [26] and Sattinger [22] give information on the symmetry and properties of the 3-j symbols.

We will see that structures which are related to the cubic system (tetrahedron, cube, octahedron, FCC, BCC, etc.,) have the same magnitudes of the W invariants up to $l = 10$ and also present considerable signals in $l = 4$ and $l = 8$. Structures which are related to icosahedral symmetry (icosahedron, dodecahedron, etc.,) are characterised by high magnitudes in $l = 6$ (see five fold symmetry in fig. 1e).

5. Z invariants

What we have called the Z invariants involve a quadruple sum with two Wigner symbols:

$$\begin{aligned} Z_l = &\sum_{m_1+m_2+m_5=0} \sum_{m_3+m_4-m_5=0} (-1)^{l-m} \begin{pmatrix} l & l & l \\ m_1 & m_2 & m_5 \end{pmatrix} \begin{pmatrix} l & l & l \\ m_3 & m_4 & m_5 \end{pmatrix} \\ &\times [Q_{l,m_1} Q_{l,m_2} Q_{l,m_3} Q_{l,m_4}] / [Q_l^4] \,. \end{aligned}$$

The derivation of the last expression came from discussions with Prof. Eliot Leader (Birkbeck College, University of London). The Z_l invariants thus correspond to $m_1 + m_2 + m_3 + m_4 = 0$.

The Q, W and Z invariants have the following characteristics. (1) Each is real. (2) The Q_l invariants are always positive and are zero for odd values of l if the system is centrosymmetric. (3) The W_l invariants may be positive or negative and vanish for odd l. (4) The Z_l invariants are all positive and vanish for odd l. (5) $Q_0, W_0, Z_0 = 1$ as a result of the averaging over atoms.

6. Testing

The algebra and the programs for calculating the invariants were checked by repeating the calculations of Steinhardt et al. for exact geometric figures (cube, octahedron, f.c.c. and h.c.p. packings). They agreed closely. It was also verified that the invariants were indeed invariant with respect to the rotation of irregular test objects. These calculations were done in double precision but when using data on real Ca–O coordination polyhedra single precision was sufficient. Calculations were done on a personal computer which limited the use of still higher order invariants which required a faster machine. Q, W and Z invariants were calculated up to $l = 12$.

7. Discrimination

It is of interest to record the invariants for a number of standard geometrical objects to estimate the discrimination of shape and symmetry (see table 1).

7.1. INVARIANTS FOR STANDARD GEOMETRICAL OBJECTS

In real structures the CP are not perfectly symmetric and it is important to have a reference in order to establish how far the polyhedron is from being "perfect". For this reason, the invariants for standard geometrical objects should

Table 1
W_l Invariants for standard geometrical objects.

Polyhedron	W_2	W_4	W_6	W_8	W_{10}	W_{12}
tetrahedron	–	−0.159317	1.31606E–2	5.8454E–2	−9.01302E–2	2.8806E–2
octahedron	–	0.159317	1.31606E–2	5.8454E–2	9.01302E–2	2.3946E–2
cube	–	−0.159317	1.31606E–2	5.8454E–2	−9.01302E–2	2.8806E–2
icosahedron	–	–	−0.16975	–	−9.3968E–2	9.9039E–2
dodecahedron	–	–	0.16975	–	−9.3968E–2	−9.9039E–2
cuboctahedron	–	−0.159317	−1.31606E–2	5.8454E–2	−9.01302E–2	8.7390E–2
HCP 12at	–	0.134097	−1.24419E–2	5.12959E–2	−7.9850E–2	0.5065E–2
BCC 14at	–	0.159317	1.31606E–2	5.8454E–2	−9.01302E–2	−4.9573E–2
pent-bipyramid	0.239045	0.13409	−9.3059E–2	7.1229E–2	9.0242E–2	8.46E–2
square	0.239045	0.12497	−7.2146E–2	6.38E–2	−1.6309E–2	4.2356E–2

be calculated. The structures considered as standard include the Platonic solids (tetrahedron, octahedron, cube, icosahedron and dodecahedron), the cuboctahedron (FCC), the BCC (15 atoms), the pentagonal bipyramid, pentagon, square, equilateral triangle and a single random vector (see figs. 2 and 3). The idea of this section is to analyze the important features presented by these structures using the invariants.

The information obtained from the clustering program is represented in tree diagrams or dendrograms in which the length of the horizontal lines indicate how similar are two structures. For example, in fig. 4a the tetrahedron and the cube do not have horizontal distance, therefore, the invariants considered ($|W_l|$ and Z_l) are the

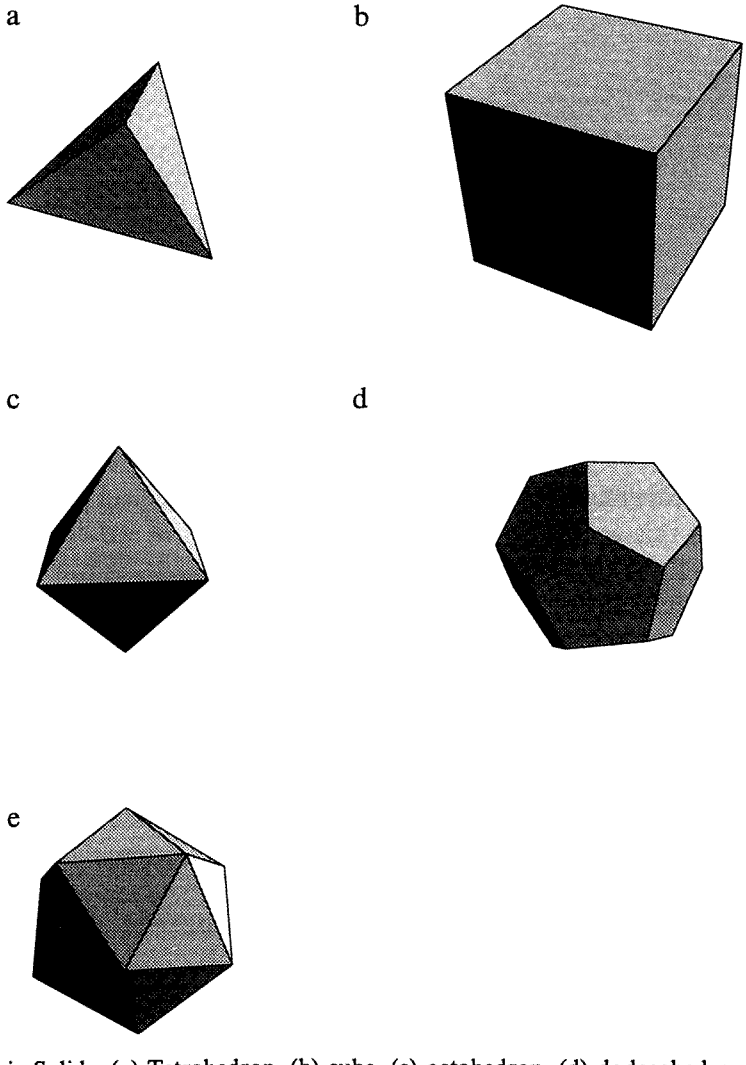

Fig. 2. Platonic Solids. (a) Tetrahedron, (b) cube, (c) octahedron, (d) dodecahedron, (e) icosahedron.

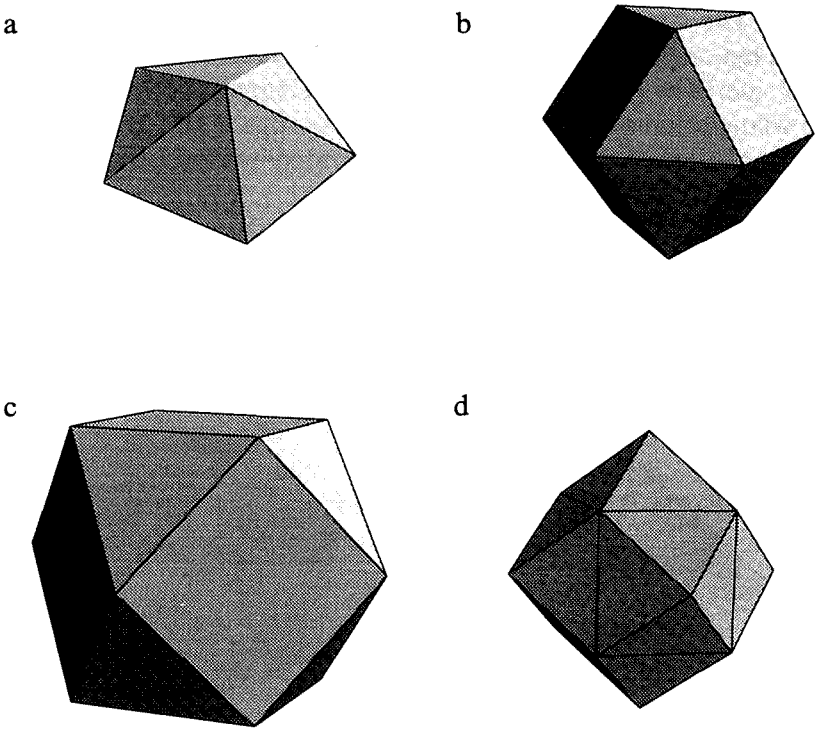

Fig. 3. (a) Pentagonal bipyramid, (b) HCP polyhedron, (c) FCC cuboctahedron, (d) BCC polyhedron.

same. The next structure to be more related to the tetrahedron and the cube is the octahedron. In this way it is possible to identify groups of structures which share similarities. In fig. 4a we get three main groups. The first is composed by the cube, tetrahedron, octahedron, and HCP polyhedra, the second, by the icosahedron and dodecahedron and the third, by the pentagon, the pentagonal bipyramid, the square, the equilateral triangle and the single random vector. In fact, The CP in the first group have symmetries compatible with the cubic system. The second group is related to icosahedral symmetries and the third contains structures with low symmetry. Therefore, using the Z and the magnitudes or absolute value of the W invariants it is possible to distinguish among certain levels of symmetry.

About the numeric values of the W and Z invariants we note the following:

1. The $|W_l|$ up to $l = 10$ are the same for cubic polyhedra (tetrahedron, cube, octahedron, FCC cuboctahedron and BCC polyhedron).
2. The values in $l = 4$ and $l = 8$ are related to cubic symmetries.
3. For the icosahedron and the dodecahedron the $|W_l|$ are the same up to $l = 12$. Having the first nonzero invariant in $l = 6$ which characterises the icosahedral symmetry.

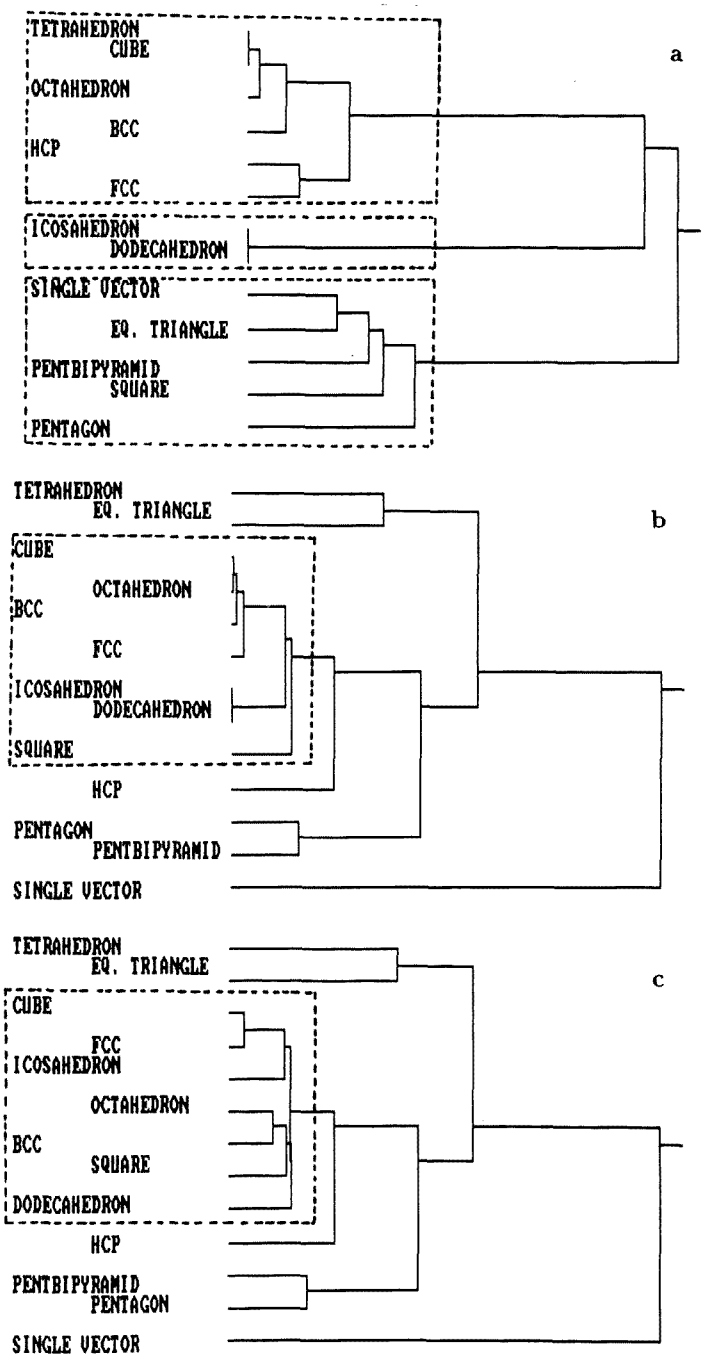

Fig. 4. (a) Tree diagram considering $|W_l|$ and Z_l invariants for ideal polyhedra. (b) Q_l for odd values of l, magnitudes of W_l and Z_l invariants for ideal polyhedra. (c) Q_l for odd values of l, W_l and Z_l invariants for ideal polyhedra. The dotted boxes indicate groups which share similarities. (a) Different kinds of symmetry. (b) Centrosymmetry. (c) Centrosymmetry.

4. The HCP polyhedron has its own characteristic invariants different from the cubic and icosahedral structures.
5. The Z_l invariants have a similar behaviour as the magnitudes of the $W_l's$. So, observations 1 to 4 can be applied to the $Z_l's$.

As we mentioned in the last section, The Q invariants for odd $l's$ determine whether or not the polyhedron is centrosymmetric. Adding this information to the characteristics in our clustering program, we are able to distinguish between centrosymmetric and noncentrosymmetric structures. For example, between the cube (centrosymmetric) and the tetrahedron (noncentrosymmetric). Otherwise, just using the W or the Z, the distinction is not possible (see figs. 4b and 4c).

8. Invariants of coordination polyhedra in intermetallic compounds

Daams et al. [4] have extracted different coordination polyhedra for intermetallic compounds from databases. The information they give is the following:

1. Fractional coordinates of the coordination polyhedra.
2. A pictorial 3-dimensional view of the coordination polyhedra.
3. The atomic environments as realized in the structure [2].

The information above is important for giving a qualitative idea of the coordination polyhedron, but using the invariants under rotation we can quantify information from the polyhedron and therefore, characterise it.

We have calculated the invariants Q, W and Z for all the 24 coordination polyhedra of the intermetallic compounds given by Daams [4].

In order to show more clearly our results, we have divided the CP of intermetallic compounds into two groups. In figs. 5a and 5b, two dendrograms with $|W_l|$ and Z_l are represented. The idea of these figures is to see how different levels of symmetry are related. We notice that all the CP are far from being icosahedral, although there are relationships among FCC and BCC packings. In figs. 6a, 6b, 7a and 7b the Q_l for odd $l's$ are introduced for analyzing centrosymmetry. These results indicate that of all 24 CP, 10 are centrosymmetric. These centrosymmetric CP are the following:

1. Cu_2Mg with Cu in the center $CN = 12$ (CuMg2 in the diagram).
2. $BaPb_3$ with Ba in the center $CN = 12$ (BaPb1 in the diagram).
3. $BaPb_3$ with Pb in the center $CN = 12$ (BaPb3 in the diagram).
4. $CaCu_5$ with Ca in the center $CN = 18$ (CaCu1 in the diagram).
5. $CaCu_3$ with Cu in the center $CN = 12$ (CaCu3 in the diagram).
6. Al_4Ba with Ba in the center $CN = 22$ (AlBa1 in the diagram).
7. $Cu_4Si_4Zr_3$ with Zr in the center $CN = 20$ (CuSi1 in the diagram).

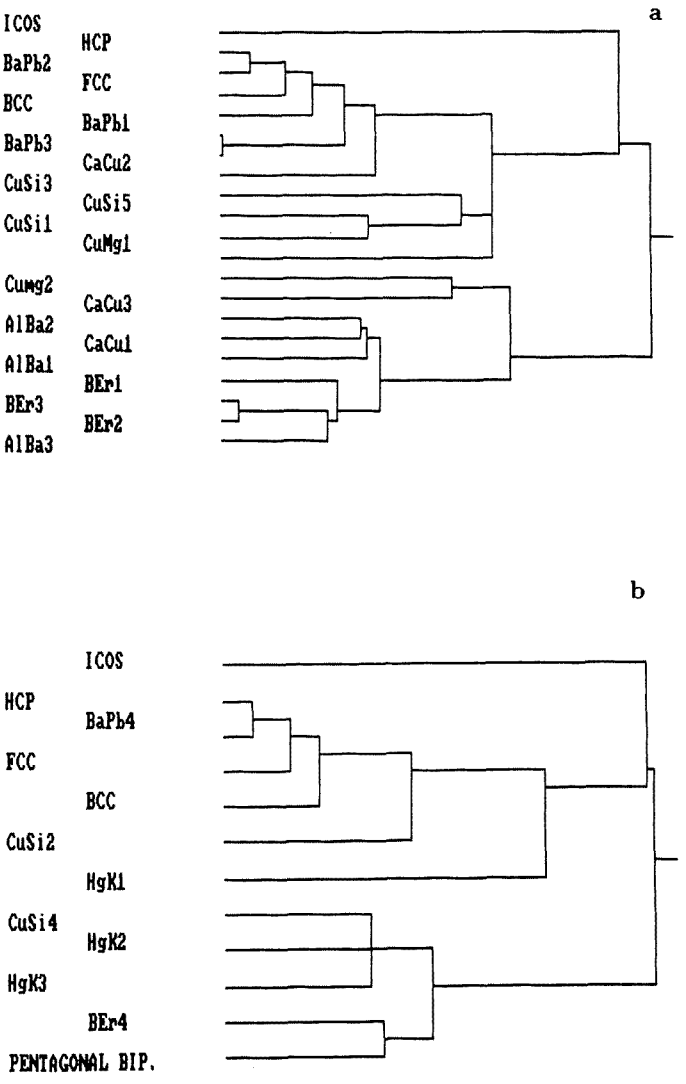

Fig. 5. (a, b) $|W_I|$ and Z_I for intermetallic compounds.

8. B_2ErIr_3 with Er in the center $CN = 20$ (BEr1 in the diagram).
9. B_2ErIr_3 with Ir in the center $CN = 14$ (BEr2 in the diagram).
10. B_2ErIr_3 with Ir in the center $CN = 14$ (BEr3 in the diagram).

The notation used in the diagrams or dendrograms includes the symbols of the elements which compose the CP and a number which identifies the different CP in the same structure. The CP are given in the same order as in Daams' classification [4].

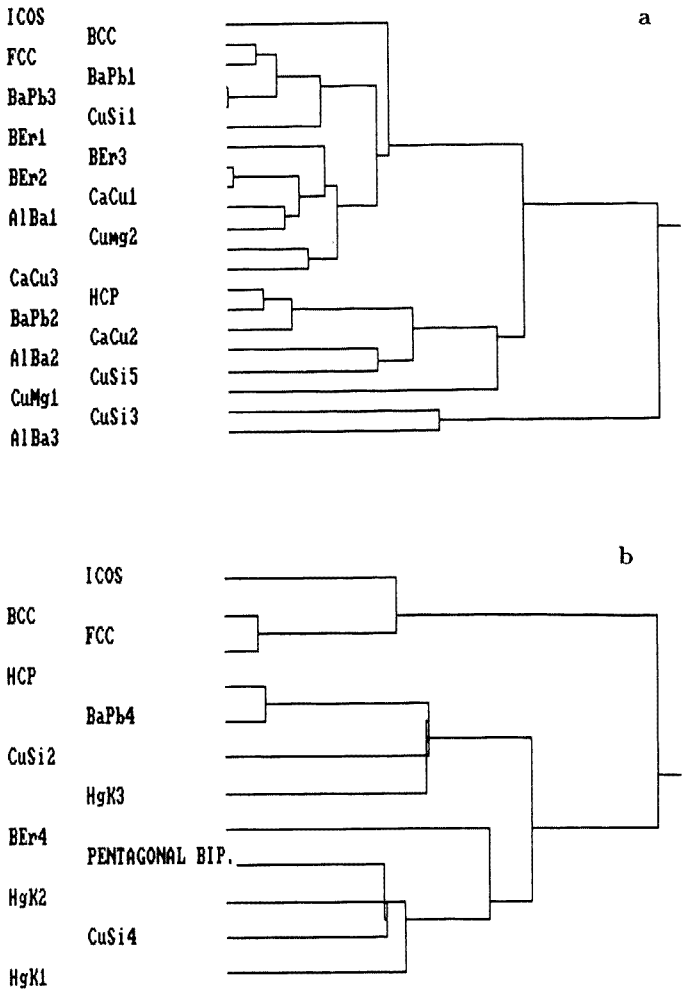

Fig. 6. (a, b) Q_l for odd values of l, Magnitudes of W_l and Z_l invariants for intermetallic compounds.

8.1. THE JAHN-TELLER EFFECT

Sometimes, the distortions in a polyhedron can be caused by non-bonding electron effects such as those due to d-electrons in transition metal compounds. One of these is know as the Jahn-Teller effect and consists in axial distortions of an octahedron [30]. Two opposite bonds of the octahedral CP are shorter or longer than the other four bonds. This effect can be studied by calculating the W_l invariants for different c/a ratios. It is important to note here that we have to consider all the 18 bounds in the polyhedron because just considering the directional coordination

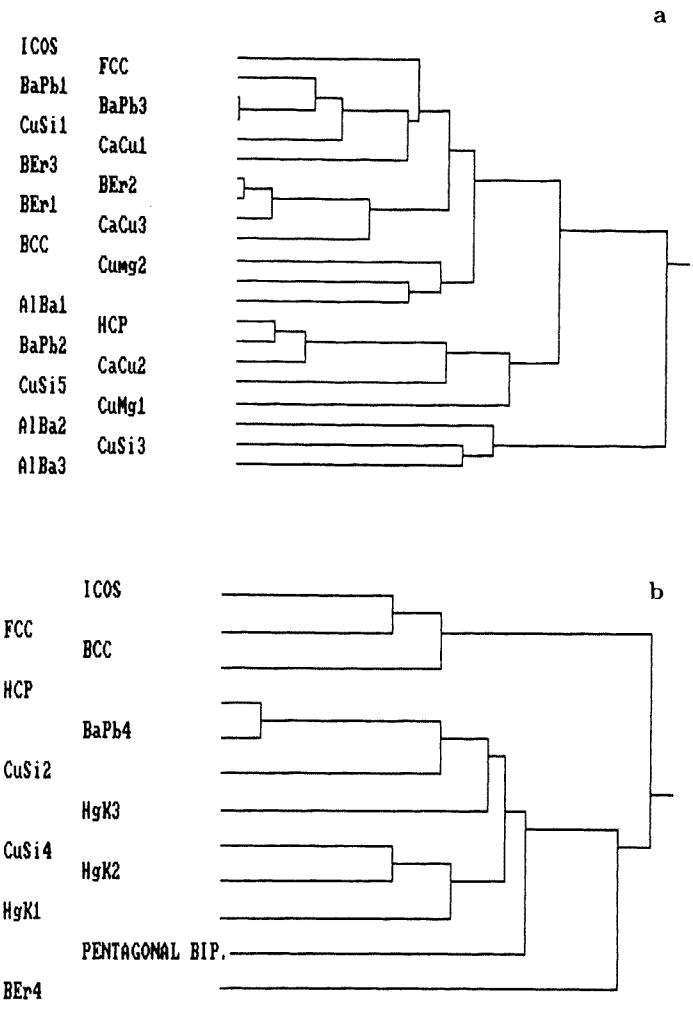

Fig. 7. (a, b) Q_l for odd values of l, W_l and Z_l invariants for intermetallic compounds.

of the central atom (6 bonds), we will not obtain information about the distortion. In our calculations, we use bond directions and not magnitudes. The results obtained are interesting for two main reasons. First, because we can measure the degree of distortion and second, because the perfect octahedron is easy to identify. In fig. 8a we can see that when the octahedron is compressed, the $W_l's$, with $l = 2$, change to positive sign and if we pull out the structure, we get a negative value. Looking at figs. 8b to 8f it is trivial to see at which values of c/a ($c/a = c'\sqrt{2}/a = 1$) we get the perfect octahedron since the most symmetric structure is characterised by a critical point, a minimum ($l = 6$), a maximum ($l = 4, l = 10, l = 12$) and an inflexion point ($l = 8$).

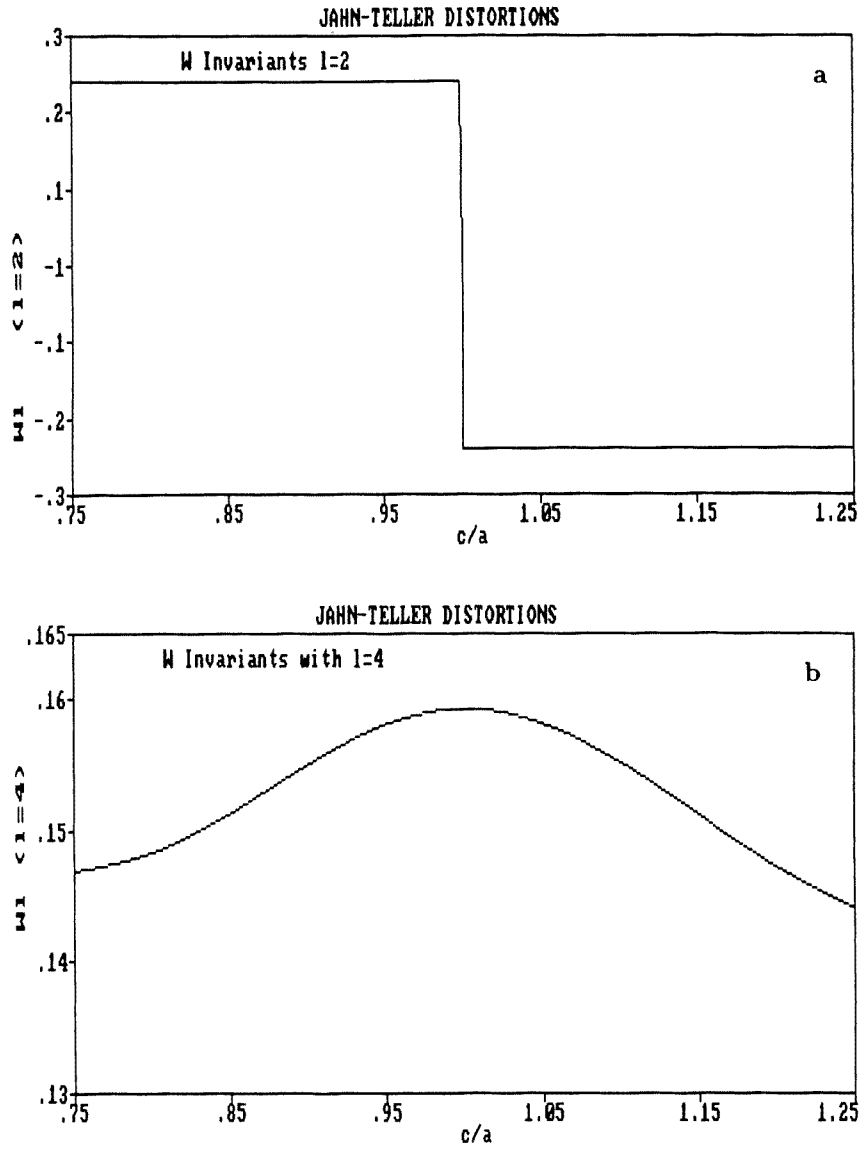

Fig. 8 (continued on next pages).

9. Ca–O polyhedra

The coordination of oxygen ions about calcium is notoriously variable, coordination numbers varying from about 5 to 9, so that it is of importance to develop a method of characterising such polyhedra from data available in the Inorganic Crystal Structure Database (ICSD), assuming that O ions are all at the same distance from the central calcium ion.

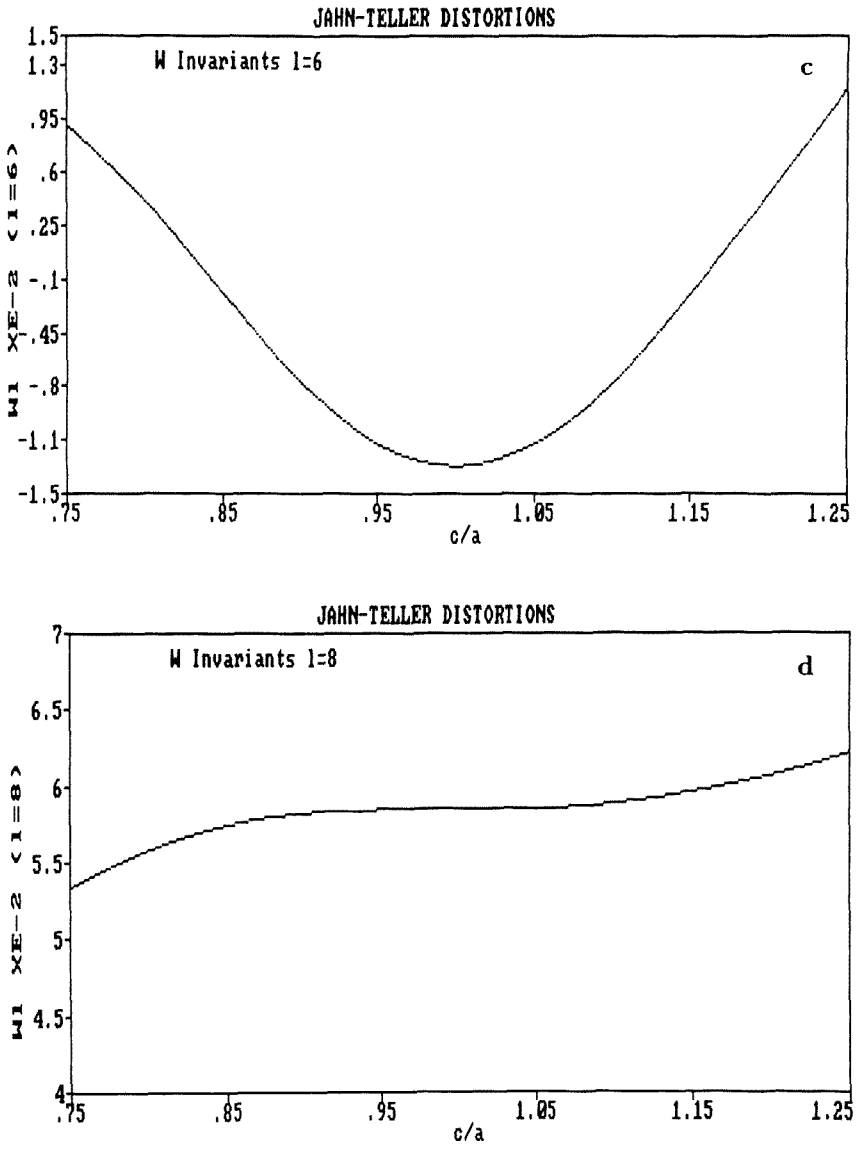

Fig. 8 (continued).

As a test invariants for a variety of Ca–O polyhedra were calculated and the results were used as data for clustering, together with invariants from standard polyhedra. This shows that various nearly regular coordination polyhedra can be picked out automatically.

Each oxygen atom was given unit weight when calculating the invariants but various weighting systems could be devised for different purposes. For example, weights proportionate to $1/r^2$ would represent the solid angles subtended by each

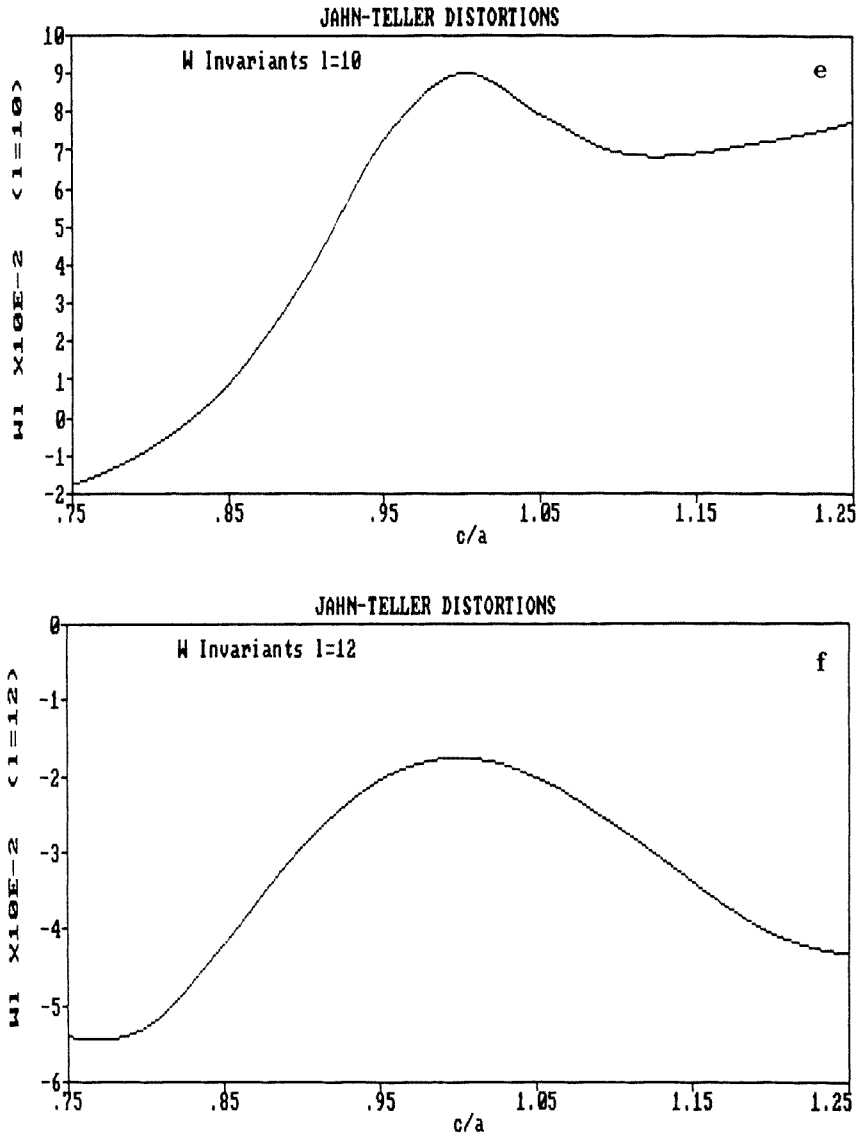

Fig. 8. (a–f) Invariants during Jahn-Teller distortions in octahedral coordination. (a) $W_l = 2$, (b) $W_l = 4$, (c) $W_l = 6$, (d) $W_l = 8$, (e) $W_l = 10$, (f) $W_l = 12$.

oxygen ion at the calcium ion. Indeed it is possible that a sum out to large distances could be made to converge if a suitable inverse power of r were used. This could show the symmetry of the electrostatic field in which the central ion was situated as in the Morse theory.

In figs. 9a, 9b and 9c, dendrograms which represent the invariants are shown. In these figures (9a, 9b and 9c), we have been consistent with the system followed in the last two sections. This means, that first we use the W_l and the Z_l invariants for

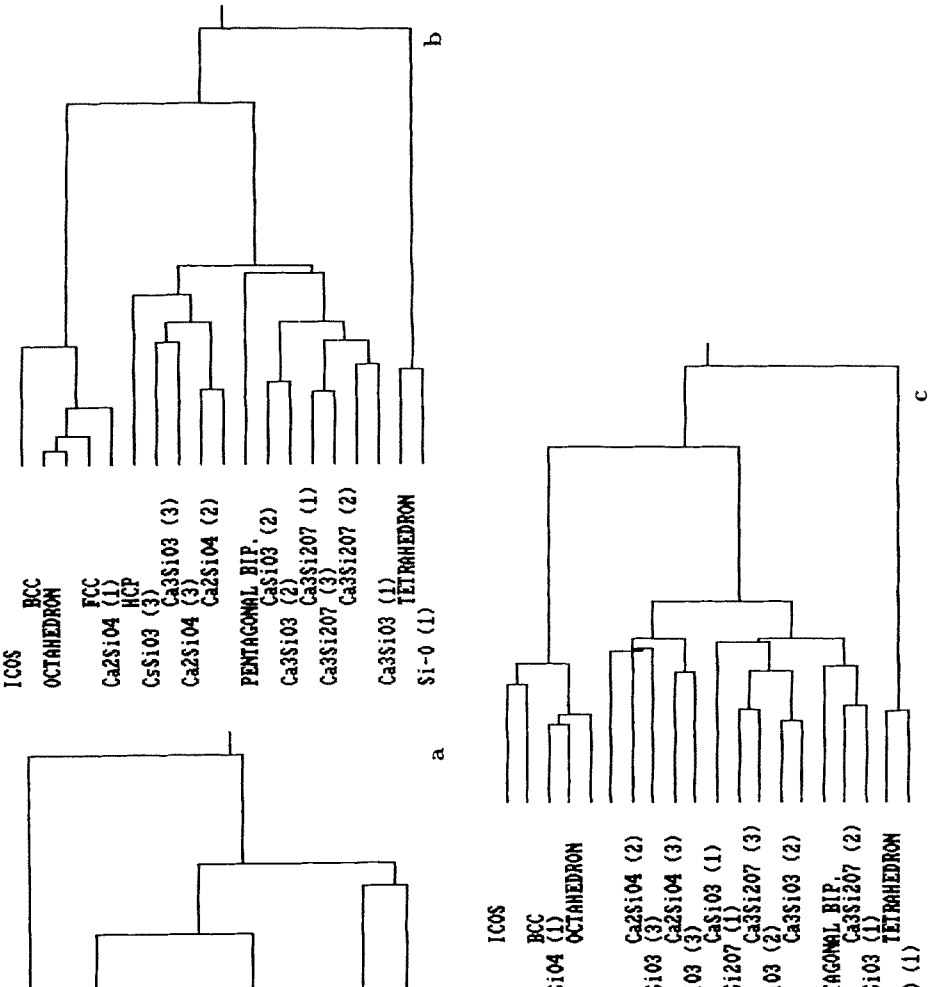

Fig. 9. (a) Z_l and magnitudes of W_l for silicates. (b) Q_l for odd values of l, magnitudes of W_l and Z_l invariants for silicates. (c) Q_l for odd values of l, W_l and Z_l invariants for silicates.

studying symmetry relations (fig. 9a) and then, the Q_l invariants are considered for analyzing centrosymmetry (see figs. 9b and 9c).

10. Clusters

The study of clusters or small aggregates is necessary in the description of atomistic models of different structures like liquids [7,1], twinned particles, quasicrystals and amorphous solids [21]. Hoare has studied stable small clusters (minimum potential energy) where non-crystalline symmetries are present [10]. In fact, in computing simulated annealing with one minimum interatomic potentials like Lennard-Jones (6-12), Morse, Lennard-Jones (4-7) etc., the symmetry which predominates is Icosahedral [27]. It is interesting to see that, depending on the size, one can find different symmetries in the same material [12]. Due to frustration effects, clusters with one kind of atoms cannot grow to "infinity", but it seems that by introducing different sorts of atoms the frustration can be alleviated to some extent [20]. Nowadays, it is common to use the Monte Carlo method (simulated annealing) and molecular dynamics to generate clusters. The most common ways for characterising these are by radial distribution, bond distribution and angular distribution [27]. The radial distribution consists in analyzing how the atoms are arranged according to their distance from the center of mass. The bond distribution uses the different distances between pairs of atoms in order to give an idea about how the bonds are present in the cluster. The angular distribution uses the angles between the bonds in the cluster. It is difficult to use these distributions to describe symmetric features of the cluster, but using the invariants we can characterise the cluster and say something about its symmetry. Therefore, the invariants can be seen as a complementary tool for studying small clusters.

The small clusters considered here were computed by simulated annealing (Monte Carlo) using the Lennard-Jones (6-12) potential (one minimum potential) [27]. In particular, for the calculation of the invariants, we use the clusters composed of 4 (tetrahedron), 7 (pentagonal bipyramid), 13 (icosahedron), 19, 23, 26 and 33 (dodecahedral) atoms since these have been reported as magic numbers in mass spectroscopy experiments with argon [5]. In fact, 7, 13, 19, 23 and 26 atom clusters present strong minima of potential energy. Other aggregates introduced are the FCC cuboctahedron and the HCP (hexagonal close packing), both with 13 atoms (see fig. 10).

In order to characterise clusters by invariants, all the first neighbour bonds in the aggregate will be taken into account. The criterion consists in considering all the bonds with distances less or equal than $1.2r_0$ [8], [25] (where r_0 is the equilibrium position in a Lennard-Jones type potential). Note that the bonds are not directed, so the Q_l for odd values of l change if we scramble the coordinates, but the even values remain the same since these are invariant under inversion. It is important to

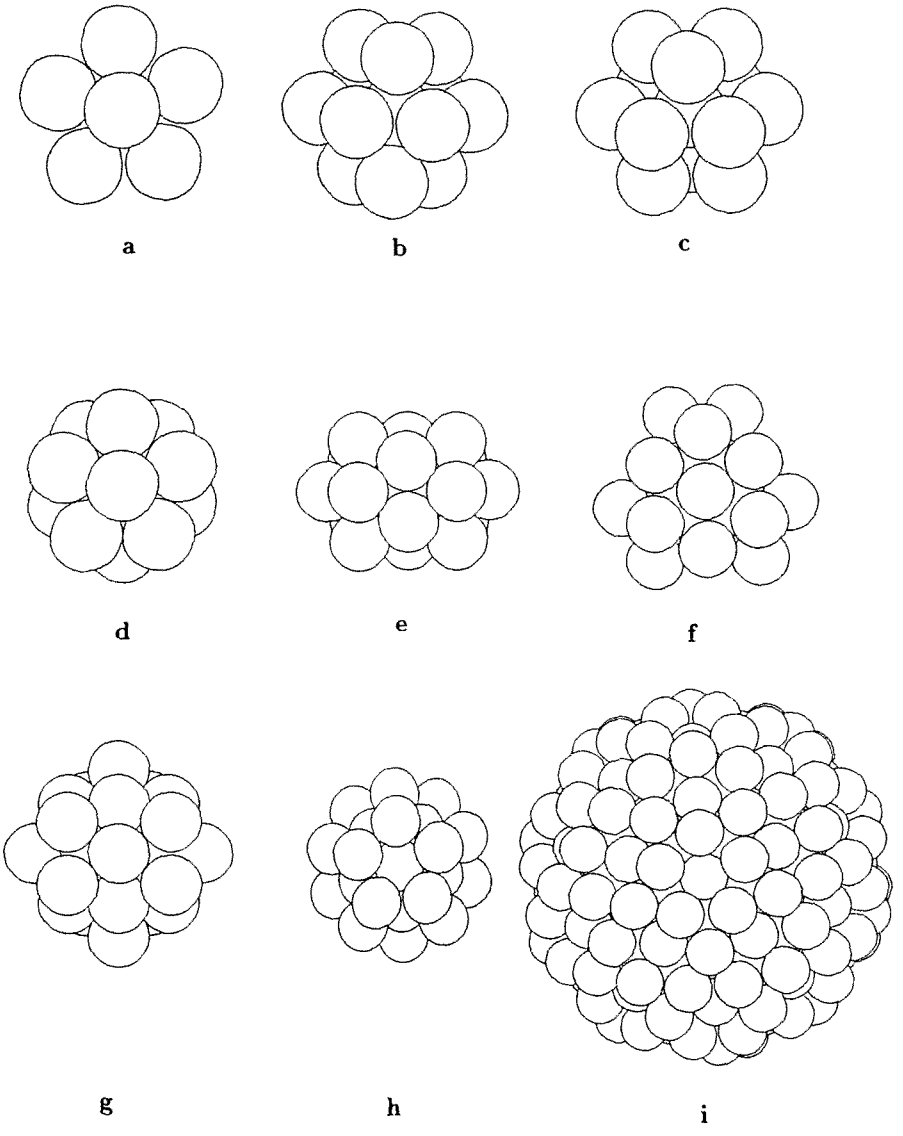

Fig. 10. (a) $N = 7$ (pentagonal bipyramid), (b) HCP $N = 13$, (c) FCC $N = 13$, (d) icosahedron $N = 13$, (e) $N = 19$, (f) $N = 23$, (g) $N = 26$, (h) $N = 33$ (dodecahedron), (i) $N = 317$ quasicrystalline cluster.

mention here that, in clusters, the surface to volume ratio is high and sometimes there is no central atom as in the case of CP (coordination polyhedra).

Using the magnitudes of the W_l invariants, the tree diagram shown in fig. 11a is obtained. Here, we can distinguish three main groups. The first is related to cubic symmetries, the second, to icosahedral symmetries, and the third, to clusters with a lower type of symmetry. With regard to the first group, it is interesting to see the

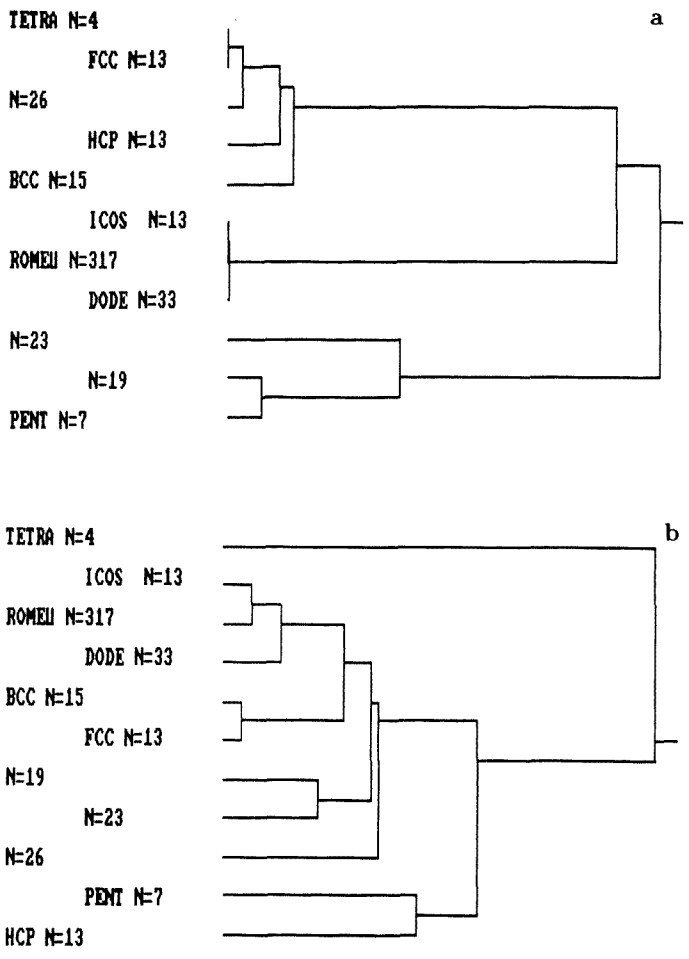

Fig. 11. (a) Magnitudes of W_l for small clusters. (b) W_l invariants for small clusters.

presence of the cluster of 26 atoms. In fact, this has tetrahedral symmetry plus mirror planes that contain 3-fold and 2-fold axes which generate 4-fold rotation reflexion axes (T_d or $\bar{4}3m$). In the second group, the icosahedron $N = 13$, the Romeu $N = 317$ and the dodecahedral $N = 33$, all present icosahedral symmetry. The $N = 317$ cluster is proposed by Romeu [20] as quasicrystalline model with icosahedral symmetry. Therefore, this agrees with the results obtained from the invariants. Finally, in the third group composed by the $N = 7$ pentagonal bipyramid (decahedron), the $N = 19$ and the $N = 23$, we see that a common feature is that all have low symmetries and are formed by an exact number of decahedra 1, 3 and 4, respectively.

In fig. 11b the signs of the $W_l's$ are included with the main idea of discriminating among some estructures with the same magnitudes (same symmetry) as in the case of the icosahedral clusters, and the FCC and tetrahedron.

10.1. THE CUBOCTAHEDRON–ICOSAHEDRON TRANSITION

In 1962, Mackay [17] studied an icosahedral packing of equal spheres and its transformation into a cuboctahedral array of atoms (a cubic close-packed assembly) pointing out the possibility of natural occurrence of the icosahedral clusters. In fact, there is experimental evidence of the cuboctahedron–icosahedron transition in small gold particles and argon clusters [12], [6] and [16].

According to energy calculations with a Lennard-Jones potential, icosahedral clusters are more favorable than cuboctahedral clusters [29], but there is a critical size at which cuboctahedral structures start to be more stable. Some authors [29,6,16] have suggested that the icosahedral–cuboctahedral (fcc-crystalline) transition takes place at sizes between 3000 and 4000 atoms.

We have studied how the $|W|$ invariants change when the symmetry changes by calculating the invariants under rotation during different stages of the transition process (see figs. 12 and 13). Signals in $l = 4$ and $l = 8$ decrease and signals in $l = 6$ and $l = 10$ increase. Note that high values in $l = 4$ and $l = 8$ are characteristic of cubic assemblies, and high values in $l = 6$ and $l = 10$ are representative of icosahedral symmetry.

11. Maxwell's theory of invariants

J.C. Maxwell showed [11] that spherical harmonics Y_m^n, which are designed to be solutions of Laplace's equation $\nabla V = 0$, can be equivalently represented as the superposition of the potentials due to charge dipoles at the origin. For example, the tesseral harmonic Y_m^n can be produced by $n - m$ dipoles along the z axis and m others distributed in the equatorial plane at angular intervals of π/m.

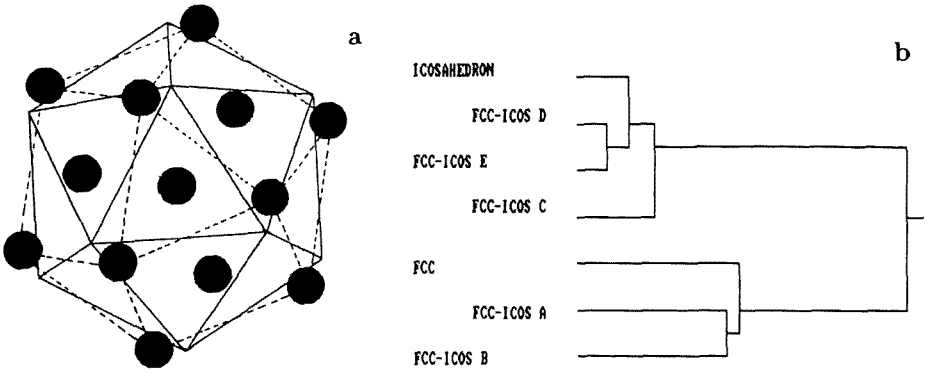

Fig. 12. (a) The cuboctahedron–icosahedron transition, (b) tree diagram showing the invariants during different stages of the transition.

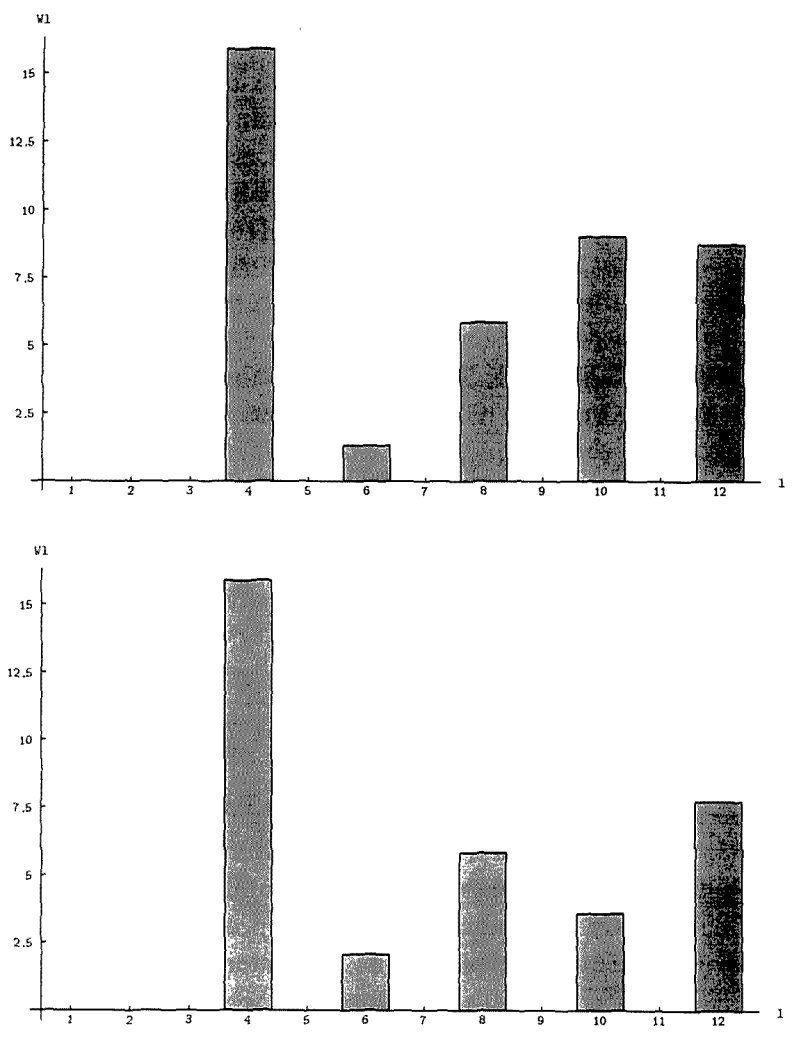

Fig. 13 (continued on next pages).

In a way, the Ca–O polyhedra, regarded from a sufficient distance, are themselves materealizations of such aggregates of dipoles.

It might be further investigated whether the invariants can be found to be combinations of the invariants of standard regular polyhedra and looked up on as superposed waveforms.

12. Conclusion

It has been shown that the invariants under rotation provide useful information

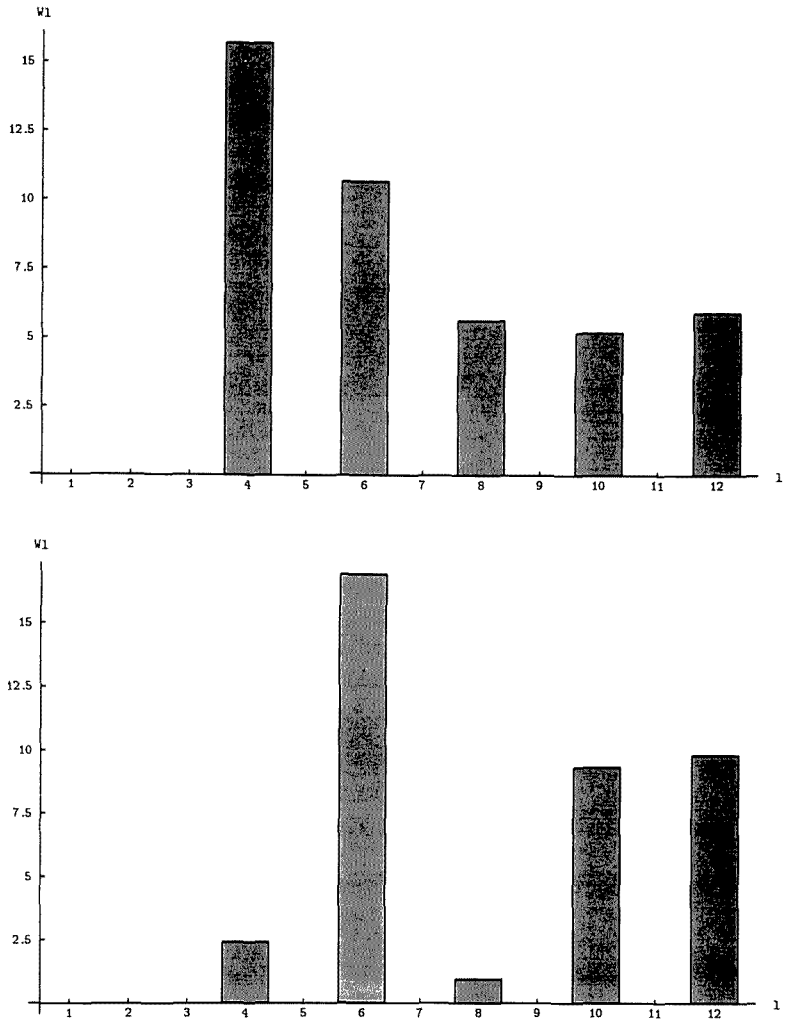

Fig. 13 (continued).

for characterising coordination polyhedra and clusters. Due to the sensitivity of these invariants it is possible to differentiate between symmetric and slightly distorted structures, and also to establish common features related to the symmetry and shape of different arrangements of atoms. On the other hand, important characteristics of the structures studied have been obtained by using a simple clustering algorithm which considers the invariants as input data. Since the necessary information for calculating the invariants can be found in data bases like the Inorganic Crystal Structure Data Base (ICSD), it is possible to establish an automatic way for characterising, quite efficiently, a great number of structures.

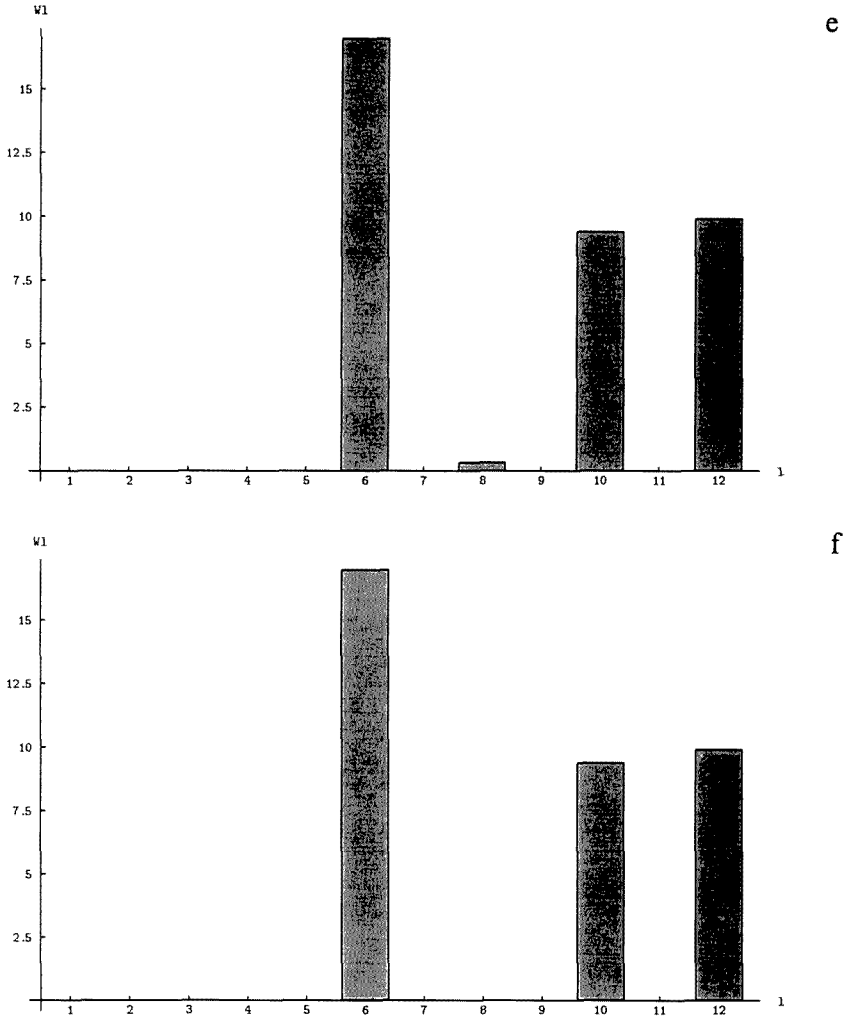

Fig. 13. Histograms with the magnitudes of W_l during the transition. (a) FCC cuboctahedron. (b) FCC-ICOS A. (c) FCC-ICOS B. (d) FCC-ICOS C. (e) FCC-ICOS D. (f) Perfect icosahedron.

Acknowledgements

We are grateful to Prof. Elliot Leader (Department of Physics, Birkbeck College) for fruitful discussions on the Z invariants. One of us (H.T.) is very grateful to Dr. Jacek Klinowski of the Chemistry Department of Cambridge University for his invitation to collaborate in his group, for allowing computing facilities and for financial support. Part of this work was given in a lecture at a conference on "Coordination Polyhedra" in Bielefeld, Germany, in February 1991. The programs for calculating the invariants and tables for different structures are available for those interested.

References

[1] J.D. Bernal, Proc. Roy. Soc. London A 280 (1964) 299.
[2] G.O. Brunner and D. Schwarzenbach, Z. Kristallogr. 133 (1971) 127.
[3] H.-J. Bunge, *Texture Analysis in Materials Science* (Butterworths, London, 1982) p. 593 (*in German*, Akademie-Verlag, Berlin, 1969).
[4] J.L.C. Daams, Structure type atlas, to be published by the American Society for Metals.
[5] O. Echt, K. Sattler and E. Recknagel, Phys. Rev. Lett. 47 (1981) 1121.
[6] J. Farges, M.F. Feraudy, B. Raoult and G. Torchet, Surf. Sci. 106 (1981) 95.
[7] J.L. Finney, Comput. Math. Appl. 17 (1989) 341.
[8] F.C. Frank, Proc. Roy. Soc. London A 215 (1952) 43.
[9] H. Hauptman, Angew. Chemie 25 (1986) 603; Science 233 (1986) 178.
[10] M.R. Hoare, Ann. N.Y. Acad. Sci. 279 (1976) 186; J. Non-Cryst. Solids 31 (1978) 157.
[11] E.W. Hobson, Spherical harmonics, Encycl. Brit. (11 Ed.) Vol. 25, pp. 649–661.
[12] S. Iijima, Phys. Rev. Lett. 56 (1986) 616.
[13] M.V. Jaric, Orientational order and quasicrystals, in: *Bond Orientational Order in Condensed Matter Systems*, ed. K.J. Strandburg (Springer, Berlin, 1992).
[14] J. Karle, Angew. Chemie 25 (1986) 614.
[15] L.D. Landau and E.M. Lifshifts, *Quantum Mechanics* (Pergamon, New York, 1965).
[16] W. Lee and G.D. Stein, J. Phys. Chem. 91 (1987) 2450.
[17] A.L. Mackay, Acta Cryst. 15 (1962) 916.
[18] T.M. MacRobert, *Spherical Harmonics* (Methuen, London, 1927).
[19] W.H. Press, B.P. Flannery, S.A. Teukolsky and W.T. Vetterling, *Numerical Recipes* (Cambridge Univ. Press, 1986).
[20] D. Romeu, Int. J. Mod. Phys. B2 (1988) 77.
[21] D. Romeu, Acta Metall. Mater. 38 (1990) 113.
[22] D.H. Sattinger, J. Math. Phys. 19 (1978) 1720.
[23] N.J.A. Sloan, *A Handbook of Integer Sequences* (Academic Press, London, 1973).
[24] R. Spencer, Byte (Sept. 1984) p. 129.
[25] P.J. Steinhardt, D.R. Nelson and M. Ronchetti, Phys. Rev. B28 (1983) 784.
[26] J.D. Talman, *Special Functions, a Group Theoretic Approach*, Math. Phys. Monograph Ser. (Benjamin, New York, 1968).
[27] H. Terrones, B.Sc. Thesis, Universidad Ibero-americana, México D.F. (1986).
[28] B.K. Vainshtein, L.A. Feigin and D.I. Svergun, Acta Phys. Acad. Sci. Hung. 53 (1982) 105.
[29] B.W. Van der Waal, J. Chem. Phys. 90 (1989) 3407.
[30] A.R. West, *Solid State Chemistry and its Applications* (Wiley, New York, 1985).
[31] Y. Wu, B.F. Chmelka, A. Pines, M.E. Davies, P.J. Grobet and P.A. Jacobs, Nature 346 (1990) 550.